THE RECOVERY OF BUFFERED TELEMETRY DATA FOR FUTURE LOW COST SPACE MISSIONS*

Haiping Tsou, Alexander Milcant, Robert Lee and Sami Hinedi
Jet Propulsion Laboratory
California Institute of Technology
Pasadena, CA 91109,

ABSTRACT: It is clear that the cost efficiency is becoming a major driver in future space missions. Because of the constraints 011 total cost, including design, implementation and operation, future spacecrafts arc limited in terms of their size, power and complexity. Consequently, it is expected to have future missions operate on marginal spat.c-to-grouIld communication links which, in turn, can pose an additional risk 011 the successful scientific return of these missions. For low data rate and low downlink margin missions, the concept of buffering telemetry signal for further signal processing to improve data return has been widely adopted. This paper describes techniques used for post-processing of buffered telemetry signal segments (called gaps) to recover data lost during acquisition and resynchronization. Two methods, one for closed-loop and the other one for open-loop configuration, arc disc. ussed in this paper. Both of them can be used in either forward or backward processing of signal segments, depending on where a gap is specifically situated in a pass.

1 Introduction

It is clear that the cost efficiency is becoming a major driver in future space missions. Because of the constraints 011 total cost, including design, implementation and operation, future spacecrafts arc limited in terms of their size, power and complexity. Consequently, it is expected to have future missions operate 011 marginal space-to-ground communication links. As a result, data compression techniques aboard the spacecraft, and other advanced signal processing techniques on the ground arc important to provide alternatives to increase the scientific return of a mission by improving the communication link margin. One widely adop ted concept of buffering telemetry signal for further signal processing to improve data return for low data rate and low downlink margin missions is first implemented as the Buffered Telemetry Demodulator (BTD) to support NASA's Galileo Mission [I]. In this mission, Galileo spacecraft has to rely on its low gain antenna to transmit data from Jupiter back to Earth, because of a malfunctioning high gain antenna. The low-gain antenna can only support very low symbol signal-to noise (ranging from -10 dB to -6 dB) at low symbol rates (up to 640 symbols per scc.end). It is estimated, for such a low signal-to-noise range, that the signal acquisition (including carrier, subcarrier, and symbol) can take up to ten minutes when single antenna is used. Furthermore, in order to maximize the data return, several data rate changes intending to take advantage of all the available antenna aperture 011 the ground can occur in a pass and each may require re-acquisition of the signal. The combination of the above two can result in significant data loss if signal is not buffered.

With the data buffered, various non-real-time (non-causal) signal processing techniques can be performed to reduce the data loss due to acquisition, resynchronization and loss-of-lock. For example, playing with different loop configuration such as using different loop bandwidth and/or different quadrature windowing may realize better acquisition per formance [2]. In this paper, we will focus on techniques used for reprocessing segments of buffered telemetry signal (called gaps), by using check point information obtained from the segments of buffered signal next to the gap (called pads), to recover the lost data. This presents a unique opportunity to employ non-causal signal processing techniques for the purpose of signal detection. In section 2, the brief description] of BTD and the nature of gaps arc given. Two methods, one for closed-]oo]) and the other one for open-loop configuration, arc discussed in section 3 and 4, respectively. Both of them can be used for either forward or backward gap processing, depending 011 where a gap is specifically situated in a pass. The overall gap processing strategy is discussed in section 5.

● '1'IIc research described in this paper was carried out by the Jet Propulsion Lal oratory, Califor nia Institute of Technology, under a contract with the National Aeronautics and Space Administration.

2 Buffered Telemetry Demodulator and Gaps

BTD is a software receiver implemented on a general purpose multi-CPU workstation. It performs acquisition and tracking functions for the carrier, subcarrier and symbol, as well as provides miscellaneous monitoring functions such as lock indicators, symbol SNR estimators, etc. It is designed to take advantage of multiple CPUs in doing several processes on different segments of digitally sampled and recorded signal simultaneously. For example, it can process real-t,illle samples forward (in terms of time) and reprocess any other segment of samples in the past at the same time. The necessity to reprocess a segment of samples arises from the following two scenarios: (1) the out-of-lock indication is detected in any one of the loops, and (2) the succeeding decoder fails to extract valid information. Both situations indicate that demodulation is not successfully performed for that segment of samples, which is called a *gap*. Typically, gaps are caused by either acquisition/reacquisition or cycle-slip in one of the three loops. Gaps due to acquisition/reacquisition can be found in the beginning of each pass and at the instants of data rate change. However, gaps due to cycle-slips are usually accompanied by the drop of loop sig]lal-to-noise ratio, and can occur randomly in a pass. In rare cases, a gap may happen as demodulated symbols are mis-handled in the data flow between BTD and the succeeding decoder. The processing of a gap to extract any valid information not available when that segment of signal samples were first processed is referred to as *gap closure process ing* (GCP).

Along its demodulation process, BTD keeps record of its internal states, including the lock indicator states, the state variables inside loop filter and numerically controlled oscillator (NCO) for all three loops. These state variables are recorded at fixed intervals and are stored as *check points*. The check point information will serve as a reference when a gap closure process is necessary. For a gap situated inside a pass, it is possible to perform the GCP by using the available check point information either prior to or after the gap. The former is referred to as the *forward gap closure processing* (FGCP) because it loads in the check point information prior to the gap and start to process the gap from the beginning towards the end; the latter is referred to as the *backward gap closure processing* (BGCP) since the gap is processed in the order of reversed time. obviously, only the FGCP can be performed when the gap is at the end of a pass, and only the BGCP can be performed when the gap is at the beginning of a pass. There is no essential difference between FGCP and BGCP except the order of signal samples processed is reversed. The exclusion of either one depends solely on the availability of sufficient check point information. Since every state variable of each check point is a random variable, it is necessary to take more than one check points to make a good estimation of states at the start of GCP. A *pad* is referred to the segment of signal samples from which all the check points used for a GCP are derived. It will be clear that the pad-to-gap size ratio plays an important role in determining the strategy of GCP.

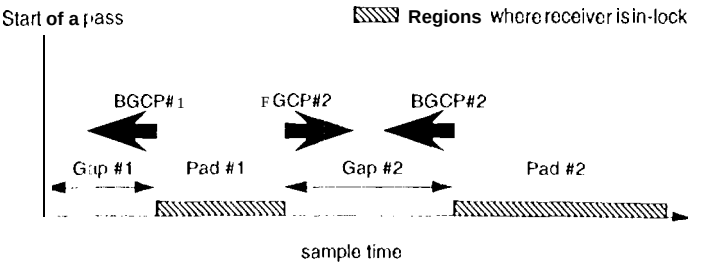

Figure 1: Conceptual Illustration of Gap Closure Processing.

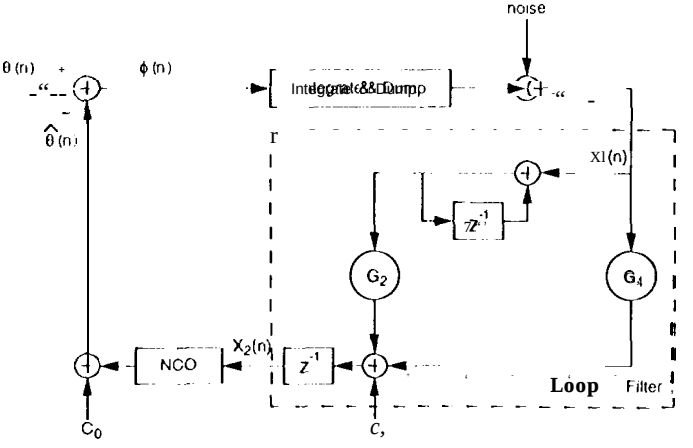

Figure 2: Augmented Second-order Digital Phase-locked Loop.

The concept of FGCP and BGCP can be simply illustrated in Figure 1, where two gaps, two pads and associated GCPs are given. The gap #1 is caused by initial acquisition at the start of a pass. It can be recovered by the BGCP #1 using check point information obtained from pad #1. The same check point information can also support the FGCP #2 in reprocessing the gap #2, where it is inside a pass and probably caused by a data rate change or an unexpected drop of loop signal-to-noise ratio. Of course, the BGCP #2 using check point information obtained from pad #2' is an alternative for the GCP of gap 7'/2.

3 Closed-Loop Gap Closure Configuration

The most straightforward way to reprocess a gap is to run the same receiver over that segment of sampled signal

with some new *a priori* information pertinent to the starting point. The *a priori* information is typically obtained by estimates of the state prior to the gap (in the case of 1(; CP) or after the gap (in the case of BGCP) in segments when the receiver is in lock. For a digital phase-locked loop (PLL), the method of loop filter coefficients initialization is first proposed to reduce the transient response [3]. For example, a second-order, baseband equivalent phase-locked loop can be augmented as shown in Figure 2. The two coefficients, C_0 and C_1, are added for the purpose of phase and frequency initialization. It is easy to snow that, at the NCO input,

$$x_2(n) = C_1 + G_1 x_1(n-1) + G_2 \sum_{i=1}^{n-1} x_1(i), \qquad (1)$$

which corresponds to the estimate of the first derivative of the incoming phase process. If the incoming phase process is assumed as

$$\theta(t) = \theta_0 + \theta_1 t + \theta_2 t^2/2, \qquad (2)$$

the steady-state phase error, in the absence of noise, becomes

$$\phi_{ss} = \frac{\theta_2 T_u}{G_2}, \qquad (3)$$

where T_u is the loop update interval. By equating (1) aud the first derivative of (2), and then substituting (3), we have

$$C_1 = 0, -\left(\frac{G_1}{G_2}\right)\theta_2 T_u + \theta_2 T_u. \qquad (4)$$

With a good *a priori* knowledge on $O.$, θ_1 and 0_2, the coefficients $C_0 = \theta_0$ and C_1 given as (4) can be used for the forward gap closure process.

The BGCP needs only a slight modification in coefficients by changing the sign in front of the terms containing θ_i, where i is a positive even integer. In our example, $C_0 = oo$ is unchanged but C_1 needs to be changed to

$$C_1 = \theta_1 + \left(\frac{G_1}{G_2}\right)\theta_2 T_u - \theta_2 T_u. \qquad (5)$$

The reason for this modification is that the odd order derivatives of a phase process do not need a sign change as the time is reversed; however, the even order derivatives do need one. This can be explained by a simple example as follows. The frequency for a periodic movement at a rate of 2π/second is always one Hertz, no matter its associated phasor is described as rotating clockwise or counter- clockwise. On the contrary, a frequency ramp increasing (positive slope) with time will be decreasing (negative slope) when the time is reversed.

4 Open-Loop Gap Closure Configuration

A gap can be reprocessed without, the use of a PLL to adaptively estimate the signal phase, provided that the signal phase is reasonably stable or slowly varying in that gap. The open-loop gap closure configuration uses an estimated phase profile to serve as the reference phase. The estimated phase profile can be obtained from the phase observation over an adjoint region where phase has been successfully tracked

It is assumed that the measurements at the output of the NCO can be modeled as

$$y(k) = \theta(k) + \nu(k) = \{\theta_0 + \theta_1 (KT) + \theta_2 (KT)^2/2\} + \nu(k), \qquad (6)$$

where $\theta(k)$ is the input phase process sampled at the interval T, and $\nu(k)$ is a zero mean Gaussian random variable with variance σ. Given m noisy correlated samples of $y(k)$, the]casl-squared estimate of the input phase parameters, namely θ_0, θ_1, and θ_2, is easily shown as [4]

$$\hat{\underline{\theta}} = \left[H^T H\right]^{-1} H^T \underline{y}, \qquad (7)$$

where $\hat{\underline{\theta}}$ is the estimation vector and $\underline{y}$ is the measurement vector given as

$$\hat{\underline{\theta}} = \begin{bmatrix} \hat{\theta}_0 \\ \hat{\theta}_1 \\ \hat{\theta}_2 \end{bmatrix} \quad and \quad \underline{y} = \begin{bmatrix} y(1) \\ y(2) \\ \vdots \\ y(m) \end{bmatrix},$$

and the observation matrix H is given as

$$H^T = \begin{bmatrix} 1 & 1 & \cdots & 1 \\ T & 2T & \cdots & mT \\ T^2/2 & (2T)^2/2 & \cdots & (mT)^2/2 \end{bmatrix}.$$

Therefore, the estimated phase at time t will be

$$\hat{\theta}(t) = \hat{\theta}_0 + \hat{\theta}_1 t + \hat{\theta}_2 t^2/2, \qquad (8)$$

which is au unbiased estimate with variance

$$\sigma^2_{\hat{\theta}}(t) = \sigma^2_y \left[p_{11} + p_{22}t^2 + p_{33}t^4/4 + 2(p_{12}t + p_{13}t^2/2 + p_{23}t^3/2)\right]), \qquad (9)$$

where p_{ij} is the (i,j)th component of the covariance matrix

$$P = \left[H^T H\right]^{-1} H^T R H \left[H^T H\right]^{-1},$$

with $R = E\{\underline{\nu}\underline{\nu}^T\}$ being the covariance matrix of the NCO output, determined by sampling the correlation function of the phase process given in [5].

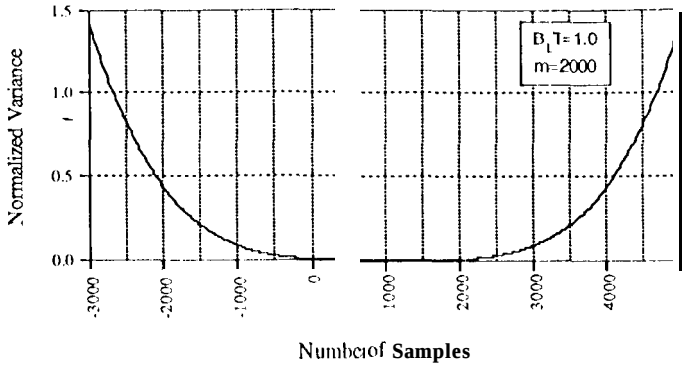

Figure 3: Performance of Least-Squares Smoother/Predictor.

B_LT	1.0	0.2	0.1	0.05	0.01
$m=100$	38.00%	14.00%	5.00%	0.00%	0.00%
$m=500$	80.80%	43.60%	29.60%	18.20%	0.00%
$m=1000$	105.00%	60.40%	43.80%	29.80%	6.20%
$m=2000$	133.85%	80.55%	60.65%	43.90%	15.05%
$m=5000$	180.62%	113.32%	88.12%	66.84%	29.94%
$m=10000$	223.91%	143.71%	113.64%	88.17%	43.92%
$m=15000$	252.95%	164.12%	130.79%	102.57%	53.41%
$m=20000$	275.43%	179.92%	144.07%	113.72%	60.76%

Table 1: The $\eta(m, B_LT)$ Values

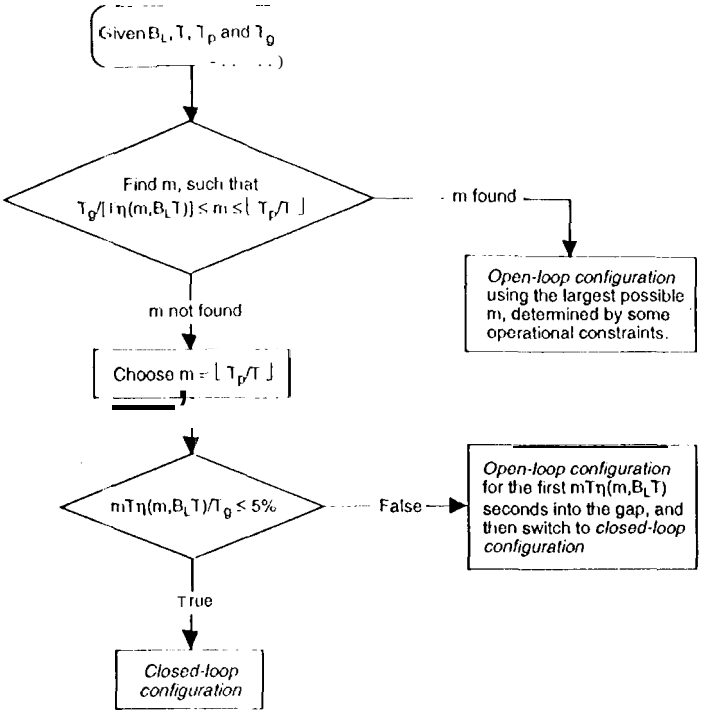

Figure 4: The overall Gap Closure Strategy.

It is interesting to note that the normalized variance of the open-loop, least-squared estimated phase, defined as the ratio of $\sigma^2_{\hat{\theta}}(t)/\sigma^2_y$, serves as an important indicator showing whether the open-loop configuration] out-performs the closed-loop configuration or not,. A ratio smaller than one actually implies that the open-loop estimated phase has smaller variance than the NCO output phase derived from the closed-loop configuration. Figure 3 gives a typical example of the performance of the least-squares smoother/predictor versus the sample number away from the observed sample one. **Note** that the region where normalized variance is less than unity extends both sides symmetrically beyond the observation window. The ratio of the single-side extension size to the observation window size, denoted as $\eta(m, B_LT)$, is listed in 'I'able 1 for various B_LT products of the loop bandwidth of the counterpart closed-loop configuration and the sampling interval, and the number of observation samples m. For example, as listed in 'J'able 1 and also shown in Figure 3, the open-loop configuration should out-perform the closed-loop configuration over any gap with size up to 133% of the available observation size $m = 2000$ and $B_LT = 1$ .0.

5 Overall Gap Closure Strategy

It is shown that open-loop configuration can simply outperform the closed-loop configuration for a certain length of time into a gap, and then its performance deteriorates rapidly when further into the gap. Based upon this phenomenon, the overall gap closure strategy which optimizes the GCP performance is depicted as the flow chart shown in Figure 4.

For a given loop bandwidth B_L, check point interval 7', gap size T_g, and the available pad size T_p, the open-loop configuration is able to process the complete gap with better performance, only if there exists at least an integer number of check points, denoted as m, which satisfies

$$\frac{T_g}{T \cdot \eta(m, B_LT)} \leq m \leq \left\lfloor \frac{T_p}{T} \right\rfloor . \qquad (10)$$

The upper limit of (1 O) is the number of available check points from the given pad, and the lower limit is the number of required check points to open-loop cover the whole gap. When such an m exists, the largest possible m, determined by some operational contraints, is chosen to ensure the best open-loop gap closure performance. When no such an m can be found to satisfy (10), it is still possible **to usc** open-loop configuration up to the point where the open-loop performance is going to be worse than the closed-loop performance, namely the first $mT \cdot \eta(m, B_LT)$ scc.ends into the gap, and then close the loop for the rest of the gap. A decision needs to be made here to justify the benefit to include additional switching mechanism from open-loop to closed-loop configuration. Typically, the break point is

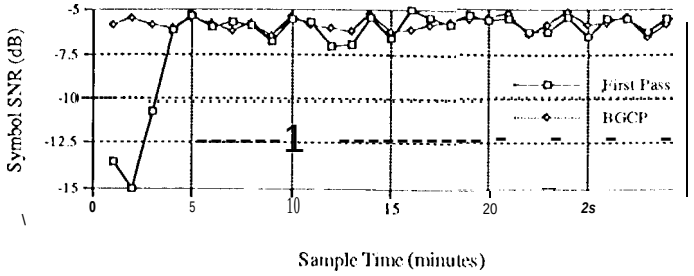

Figure 5: The Symbol SNR versus Sample Time.

arbitrarily set, as

$$\frac{mT_{1)(?)1,\ B_L,\ ?')}}{T_g} = 5\%$$

Figure 5 shows the result from GCP of a gap at the beginning of a pass. In this figure, the estimated symbol SNRs from the first BTD pass as well as the BGCP arc plotted versus sample time at one minute interval. The input signal has 1.6 Hz Doppler frequency and 0.5 mHz/sec Doppler rate, with estimated symbol SNR varying around -6 dB. It clearly shows the gap, characterized by the below-average SNR for the first three minutes in first pass, is recovered as SNR coming back to its normal level during BGCP.

6 Conclusion

The techniques used to recover any data loss from buffered telemetry signal during acquisition/reacquisition, data rate changes and cycle slips are presented in this paper. Two different configurations, one is a simple least-squares phase estimator used for open-loop gap closure process and the other involves the loop filter initialization for the closed-loop gap closure, can be chosen to rec.over lost data, depending upon the size of a gap and the size of its surrounding pad(s). Both methods have the flexibility to be used iu either forward or backward processing, which helps to c.over gaps at various position, especially at the beginning of each pass where initial acquisition) is always required. The overall strategy which optimizes the gap closure process performance is also presented. With the case for implementation 011 general purpose workstations and the flexibility to work 011 the reversed time order, these techniques should be crucial to the future low cost space missions, since the expected very low downlink communication margin is a threat to the scientific return under current ground receivers.

Acknowledgement

The authors would like to thank Ms. K. Simpson aud Mr. 'J'. Dry for their efforts in implementing the gap closure techniques in 1) '1'1). The various discussions held with Mr. J. Statman arc greatly appreciated.

References

1. H. Tsou, B. Shah, and S. Hinedi, "A Functional Description of the Buffered Telemetry Demodulator," *SUPERCOM/ICC'94*, May 1994.

2. M. Aung, W. J. Hurd, C. M. Buu, aud J. B. Berner, "The Block V Receiver Fast Acquisition Algorithm for the Galileo S-Band Mission," *TDA Progress Report 42-118, April-June 1994*, Jet Propulsion Laboratory, Pasadena, California, pp. 83-114, August, 15, 1994,

3. S. A. Stephens and J. B. Thomas, "Controlled-root Formulation for Digital Phase-locked Loops," *IEEE Trans. on Aerospace and Electronic Systems*, Vol. 30, No. 4, Oct. 1994.

4. 11. W. Sorenson, "*Parameter Estimation*," New York: M. Dekker, 1985.

5. A. Milcant and S. Hinedi, "Costas Loop Lock Detection in the Advanced Receiver," *TDA Progress Report* 42-99, *July-September 1989*, Jet Propulsion Laboratory, Pasadena, California, pp. '72-89, November 15, 1989.